ENHANCED LATTICE-REDUCTION AIDED DETECTION FOR MIMO SYSTEMS

Alan T. Murray and Steven R. Weller

School of Electrical Engineering and Computer Science
University of Newcastle
Callaghan, NSW 2308, Australia
Email: {alan.murray,steven.weller}@newcastle.edu.au

ABSTRACT

Lattice-reduction-aided detection (LRAD) has been shown to considerably increase the performance of linear Multiple-Input Multiple-Output (MIMO) detection systems. In this paper, we show that conventional LRAD is inherently incompatible with the use of different modulation formats across transmit antennas or, more generally, the use of transmit power scaling. This motivates the first of two enhancements proposed in this paper, wherein we show how the MIMO channel model can be extended to cater for transmit power scaling. The second enhancement exploits temporal channel correlation to yield lattice reduction-based detectors exhibiting considerably reduced complexity. For typical mobile environments, for example, we demonstrate a complexity reduction approaching 33% on a 4×4 system, without compromising performance.

1. INTRODUCTION

With increasing sized constellations being used in conjunction with spatial multiplexing Multiple-Input Multiple-Output (MIMO) systems, the complexity of even polynomial-time detection methods can be computationally burdensome [1]. In comparison, linear detection methods increase in complexity linearly proportional to the constellation size and number of transmit antennas used. However, basic linear detection strategies suffer significantly from noise enhancement due to non-orthogonality of the channel matrix.

Lattice-reduction-aided detection (LRAD) has been identified as a way of improving the performance of linear detection strategies. LRAD performs lattice reduction (LR) on the channel matrix to find a more orthogonal set of reduced basis vectors. The Lenstra-Lenstra-Lovász (LLL) algorithm [2] is one such lattice reduction algorithm used to find this set. Performance studies suggest that lattice-reduction-aided detection and derivatives are well suited low complexity solutions when large constellations are used [1], [3].

In this paper we describe the system setup, give a brief overview of LRAD and provide a summary of the LLL algorithm in Sections 2 to 4 respectively. From here we propose two enhancements in Section 5. Firstly, in Section 5.1 we show that conventional LRAD is inherently incompatible with the use of different modulation formats across transmit antennas or, more generally, the use of transmit power scaling. We then propose a straight forward solution by showing that the MIMO channel model can be extended to cater for transmit power scaling. Secondly in Section 5.2, we show that temporal channel correlation can be exploited to yield lattice reduction-based detectors exhibiting considerably reduced complexity. This is achieved via the introduction of a new technique we call Adaptive Lattice Reduction (ALR). Finally in Section 6, this paper concludes with some open questions that will lead to future work.

2. SYSTEM MODEL AND SETUP

We use the complex-valued N_t transmit and N_r receive antenna MIMO model:

$$\mathbf{y} = \mathbf{H}\mathbf{x} + \mathbf{n}. \tag{1}$$

The n^{th} transmit antenna is mapped to the constellation set $\mathscr{A}_n$ with elements drawn from

$$\mathbb{X} = \left\{ a + ib + \frac{1+i}{2}, a, b \in \mathbb{Z} \right\}, \tag{2}$$

the complex shifted integer grid. The complex vector $\mathbf{x}$ of length N_t represents the transmitted symbols where the element $\mathbf{x}_n \in \mathscr{A}_n$ is the symbol transmitted from the n^{th} antenna. Some (but not all) constellations can be considered a subset of $\mathbb{X}$. For example, rectangular constellations such as QPSK or m-QAM can be considered a subset of $\mathbb{X}$ but not circular constellations such as 8-PSK.

The channel is modelled by $\mathbf{H}$, an N_r by N_t complex-valued matrix representing the overall channel and has elements $h_{m,n}$ complex-valued non-dispersive fading coefficients of the channel between the n^{th} transmit and the m^{th} receive antenna. Gaussian noise is represented by the length N_r vector $\mathbf{n}$ with $\mathbb{E}\{|\mathbf{n}|\} = 0$ and $\mathbb{E}\{|\mathbf{n}\mathbf{n}^{\mathrm{H}}|\} = \sigma^2$. Finally, $\mathbf{y}$ represents the vector of received symbols of length N_r.

Many works use the real decomposition of the complex-valued MIMO transmission model [4], [5]. Lattice reduction methods can operate on both real and complex integer lattices and in particular the LLL algorithm has been extended for complex lattice reduction [6].

Maximum-likelihood (ML) detection finds the vector of symbol estimates $\widehat{\mathbf{x}}$ which minimises the euclidean distance problem as follows:

$$\widehat{\mathbf{x}} = \underset{\mathbf{x} \in \mathscr{A}^{N_\mathrm{t}}}{\arg\min} \|\mathbf{y} - \mathbf{H}\mathbf{x}\|^2. \tag{3}$$

This problem is NP-hard, and the complexity is exponentially proportional to the constellation set size and number of transmit antennas. Various heuristic approaches exist which approximately solve this problem in less than exponential time. Some detectors, such as sphere detectors, typically have complexity subexponentially proportional to the constellation set size and number of antennas and whilst their complexity is suitably low for small constellations and low numbers of transmit antennas, their complexity can become considerable as either increase. Linear detection approaches have complexity proportional to the number of transmit antennas only. Linear detection approaches use the inverse of the channel to generate an estimate of the transmitted symbols.

Zero Forcing (ZF) is a linear detection method which estimates $\mathbf{x}$ by finding the least squares solution to (1). However, correlation between the columns of $\mathbf{H}$ results in significant noise enhancement during quantisation of the least squares solution.

3. LATTICE REDUCTION AIDED DETECTION (LRAD)

The channel matrix $\mathbf{H}$ can be considered a generator matrix for the lattice $\mathbf{H}\mathbb{X}^{N_\mathrm{t}}$ of which the received symbols are elements. As such, MIMO detection can be considered equivalent to the closest lattice point problem. From lattice theory, methods exist which attempt to reduce noise enhancement. Lattice basis reduction [7, §2.6.1] does this by finding a more orthogonal set of basis vectors using the following steps adapted from [5] and detailed in [8]:

1. Find reduced lattice basis
2. Use pseudoinverse of reduced basis to form estimates
3. Quantise estimates to $\mathbb{X}$
4. Transform result to find transmitted constellation points

The reduced lattice basis is found by optimising the generating matrix, in this case the channel matrix. Complex integer linear combinations of the column vectors of $\mathbf{H}$ are taken to form the closer to orthogonal reduced matrix $\mathbf{H}_\mathrm{L}$ which spans the same set of points $\mathbf{H}\mathbb{X}^{N_\mathrm{t}} \equiv \mathbf{H}_\mathrm{L}\mathbb{X}^{N_\mathrm{t}}$ and so

$$\mathbf{H}_\mathrm{L} = \mathbf{H}\mathbf{T} \text{ or } \mathbf{H} = \mathbf{H}_\mathrm{L}\mathbf{T}^{-1}, \tag{4}$$

where $\mathbf{T}$ is a unimodular matrix with complex integer entries and $\det(\mathbf{T}) = \pm 1$, therefore $\mathbf{T}^{-1}$ also contains only complex integer entries.

As in [5], by finding an equivalent and closer to orthogonal set of the basis vectors, $\mathbf{H}_\mathrm{L}$, noise enhancement is reduced when quantisation is performed. Importantly, as $\mathbf{T}^{-1}$ and $\mathbf{x}$ both contain only integer spaced entries, so does $\mathbf{T}^{-1}\mathbf{x}$ and so symbol detection or quantisation is merely rounding to the grid $\mathbb{X}$.

We can quantitatively measure the orthogonality of a matrix using metrics such as condition number or orthogonality defect. As in [9, §4.6.2], we measure the orthogonality defect of matrices using:

$$\delta(\mathbf{H}) = \frac{\prod_{k=1}^{N_\mathrm{t}} \|\mathbf{h}_k\|}{|\det(\mathbf{H})|}, \tag{5}$$

with $\delta(\mathbf{H}) \geq 1$ for all $\mathbf{H}$ and $\delta(\mathbf{H}) = 1$ if and only if the columns of $\mathbf{H}$ are orthogonal.

To assess the impact of lattice redution on orthogonality defect, we generated 10^6 randomly chosen $\mathbf{H} \in \mathbb{C}^{4\times4}$, and computed the lattice reduced $\mathbf{H}_\mathrm{L}$. In this simulation, each $\mathbf{H}$ is an independent and identically distributed (iid) Rayleigh matrix with complex Gaussian elements with zero means and unit variances. The method used to perform lattice reduction is detailed in Section 4. The orthogonality defect was found using (5) before and after lattice reduction. This gives a quantifiable method to examine the performance of lattice reduction. The result, as shown in Fig. 1, is a considerable reduction in orthogonality defect. It is this improvement that reduces noise enhancement in linear detection methods and reduces the error rate of LRAD based systems.

4. LENSTRA-LENSTRA-LOVÁSZ (LLL) ALGORITHM

In this section we review the description of a complex LLL reduction algorithm [6]. We extend this description with the purpose of bringing context to enhancements that will follow in Section 5. We define:

- $\mathscr{H}_i$ as the squared euclidean norm of the orthogonal vectors produced by the Gram-Schmidt Orthogonalisation (GSO) of $\mathbf{H}$.
- μ_{ij} as the ratio of the length of the orthogonal projection of the i^th basis onto the j^th orthogonal vector and the length of the j^th orthogonal vector.
- $\mathbf{H}_\mathrm{L}^i$ and $\mathbf{T}^i$ represent the values of the reduced basis and transform after the i^th step of the LLL algorithm
- Initially, $\mathbf{H}_\mathrm{L}^0 = \mathbf{H}$ and $\mathbf{T}^0 = \mathbf{I}_{N_\mathrm{t}}$
- k is the index of the current column of $\mathbf{H}$ being processed such that $2 \leq k \leq N_\mathrm{t}$

The LLL algorithm then consists of three steps:

1. $\mathscr{H}$ and μ are computed using a modified GSO procedure [10]
2. Size reduction aims to make basis vectors shorter and more orthogonal by asserting the condition that $|\Re(\mu_{k,j})| \leq 0.5$ and $|\Im(\mu_{k,j})| \leq 0.5$ for all $j < k$
3. Basis vectors $\mathbf{h}_{k-1}$ and $\mathbf{h}_k$ are swapped if some condition is satisfied such that size reduction can be repeated to make basis vectors shorter

Size reduction and basis vectors swapping iterates until the swapping condition is not satisfied by any pair of $\mathbf{h}_{k-1}$ and $\mathbf{h}_k$. The resultant basis is then said to be reduced. The swapping condition for LLL reduction, also called the Lovász condition, is:

$$\mathscr{H}_k < (\delta - |\mu_{k,k-1}|^2)\mathscr{H}_{k-1}, \tag{6}$$

where δ with $\frac{1}{4} < \delta < 1$ is a factor selected to achieve a good quality-complexity trade off [2].

After each swapping step, $\mathscr{H}_{k-1}$, $\mathscr{H}_k$ and some of the $\mu_{i,j}$ values needed to be updated. Techniques can be employed to minimise the number and frequency of recalculations of $\mathscr{H}$ and μ elements [10].

Example 1 *With $\delta = \frac{3}{4}$ and $\mathbf{H}_\mathrm{L}^0 = \mathbf{H}$ let:*

$$\mathbf{H}_\mathrm{L}^0 = \begin{bmatrix} 0.75 & -0.5 \\ 0.5 & -0.5 \end{bmatrix} \text{ and } \mathbf{T}^0 = \begin{bmatrix} 1 & 0 \\ 0 & 1 \end{bmatrix},$$

and from the modified GSO we have initially:

$$\mu = \begin{bmatrix} 1.0000 & 0.0000 \\ -0.7692 & 1.0000 \end{bmatrix} \text{ and } \mathscr{H} = \begin{bmatrix} 0.8125 \\ 0.0192 \end{bmatrix}.$$

Starting with columns 1 and 2, as $|\mu_{2,1}| > 0.5$, size reduction is performed on these columns adding the first column to the second and yielding the following partially reduced matrix and corresponding transform:

$$\mathbf{H}_\mathrm{L}^1 = \begin{bmatrix} 0.75 & 0.25 \\ 0.5 & 0 \end{bmatrix} \text{ and } \mathbf{T}^1 = \begin{bmatrix} 1 & 1 \\ 0 & 1 \end{bmatrix},$$

$$\mu = \begin{bmatrix} 1.0000 & 0.0000 \\ 0.2308 & 1.0000 \end{bmatrix} \text{ and } \mathscr{H} = \begin{bmatrix} 0.8125 \\ 0.0192 \end{bmatrix}.$$

Next, the Lovász condition is checked and as $\mathscr{H}_2 < (\delta - |\mu_{2,1}|^2)\mathscr{H}_1$ the two columns are swapped yielding:

$$\mathbf{H}_\mathrm{L}^2 = \begin{bmatrix} 0.25 & 0.75 \\ 0 & 0.5 \end{bmatrix} \text{ and } \mathbf{T}^2 = \begin{bmatrix} 1 & 1 \\ 1 & 0 \end{bmatrix},$$

$$\mu = \begin{bmatrix} 1.0000 & 0.0000 \\ 3.0000 & 1.0000 \end{bmatrix} \text{ and } \mathscr{H} = \begin{bmatrix} 0.0625 \\ 0.2500 \end{bmatrix}.$$

Next, size reduction is performed on the columns once more; this time by subtracting three times the first column from the second and yielding:

$$\mathbf{H}_\mathrm{L} = \begin{bmatrix} 0.25 & 0 \\ 0 & 0.5 \end{bmatrix} \text{ and } \mathbf{T} = \begin{bmatrix} 1 & -2 \\ 1 & -3 \end{bmatrix},$$

$$\mu = \begin{bmatrix} 1.0000 & 0.0000 \\ 0.0000 & 1.0000 \end{bmatrix} \text{ and } \mathscr{H} = \begin{bmatrix} 0.0625 \\ 0.2500 \end{bmatrix}.$$

This then passes the Lovász condition (6) *which then results in the algorithm terminating. It is interesting to note that (4) holds true after every step of the algorithm. This observation will be exploited in an enhancement introduced in Section 5.2.*

5. ENHANCEMENTS

5.1 Modification for Transmit Power Scaling

Whilst the constellations of different modulation formats can be modeled on the same grid $\mathbb{X}$, in practice the average symbol power is normalised to 1 such that $\mathrm{E}\{|\mathbf{x}_i|^2\} = 1$. This is especially important when different modulation formats are used on different transmit antennas. Also, transmit power scaling can also occur due to per-antenna power control.

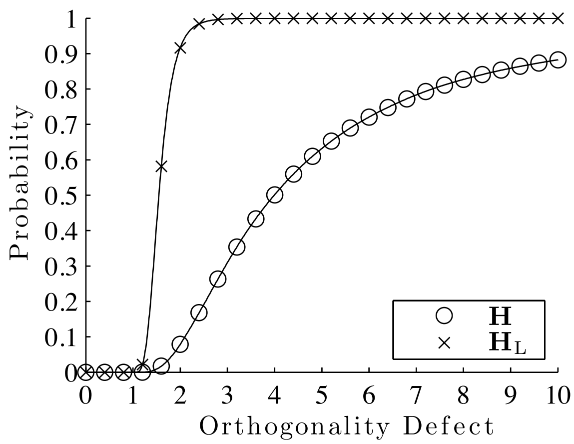

Figure 1: Cumulative density of the orthogonality defect for non-reduced and reduced basis channel matrices

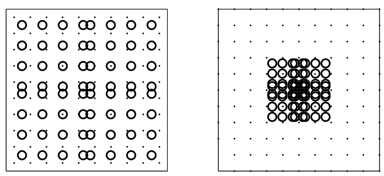

Figure 2: $\mathbf{T}^{-1}\mathbf{D}\mathbf{x}$: inverse transform of the transmitted symbol constellations (with average symbol power 1)

We can model symbol power scaling as the diagonal matrix $\mathbf{D}$ with diagonal elements d_n equal to the scaling factor for the n^{th} transmit antenna.

$$\mathbf{D} = \begin{bmatrix} d_1 & 0 & \dots & 0 \\ 0 & \ddots & & \vdots \\ \vdots & & \ddots & 0 \\ 0 & \dots & 0 & d_{N_t} \end{bmatrix}. \quad (7)$$

In the case of constellation normalisation, the elements are formed from the transmit power scalars as in the following example.

Example 2 *with QPSK on transmitter 1 and 16-QAM on transmitter 2,*

$$\mathbf{D} = \begin{bmatrix} \frac{1}{\sqrt{2}} & 0 \\ 0 & \frac{1}{\sqrt{10}} \end{bmatrix}$$

We can then incorporate this symbol power scaling into the channel model (1):

$$\mathbf{y} = \mathbf{H}\mathbf{D}\mathbf{x} + \mathbf{n}, \quad (8)$$

Unfortunately, this scaling causes problems with lattice reduction techniques as $\mathbf{T}^{-1}\mathbf{D}\mathbf{x}$ is not a subset of $\mathbb{X}$. The effects of this are shown in Fig. 2 where the inverse transform of the expected receive symbols (shown as circles) are not a subset of the grid $\mathbb{X}$ (shown as dots). As constellation points are no longer equidistant, linear quantisation is no longer possible.

In order to avoid this, we need to reverse the effect of transmit power scaling. It is not possible to simply scale the vector of received symbols as each element is a combination of transmit symbols with potentially different power scalings.

The solution proposed in this paper is to model the effect of transmit power scaling as a property of the channel rather than as a function of the transmit antenna. To do this, we scale the column vectors of the channel matrix by corresponding diagonal elements

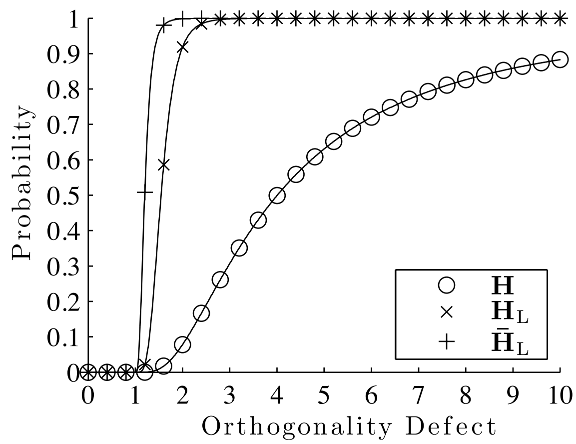

Figure 3: Cumulative density of the reduced basis orthogonality defect for non-scaled and scaled channels

of $\mathbf{D}$. Thus in (8), we perform the multiplication $\mathbf{HD}$ and perform lattice reduction on the result. We define this multiplication as $\bar{\mathbf{H}} = \mathbf{HD}$.

By incorporating transmit signal power scaling as a property of the channel, the effect is reversed when ZF is performed using the pseudoinverse of $\bar{\mathbf{H}}$ or indeed $\bar{\mathbf{H}}_{\text{L}}$. Now, the inverse transform of the expected receive symbols are once again a subset of the grid $\mathbb{X}$.

The effect of this is to increase the variance of each basis vector $\mathbf{h}_n$ by d_n^2 times. In the ZF case this results in a proportional to the increase in variance of both the received estimates and the noise amplification and so the two methods are equivalent. However, the same cannot be said in the case of LRAD.

With regards to LRAD, a reduced basis of $\bar{\mathbf{H}}$ is found using a method such as the LLL algorithm. The change in the variance of the column vectors of $\mathbf{H}$ cause a change in the reduced bases found by the LLL algorithm.

Example 3 *Using the same* $\mathbf{H}$ *from Example 1 and using the value of* $\mathbf{D}$ *from Example 2:*

$$\bar{\mathbf{H}} = \begin{bmatrix} 0.75 & -0.5 \\ 0.5 & -0.5 \end{bmatrix} \begin{bmatrix} \frac{1}{\sqrt{2}} & 0 \\ 0 & \frac{1}{\sqrt{10}} \end{bmatrix}$$
$$= \begin{bmatrix} 0.5303 & -0.1581 \\ 0.3536 & -0.1581 \end{bmatrix}$$
$$\bar{\mathbf{H}}_{\text{L}} = \begin{bmatrix} 0.0560 & -0.2141 \\ -0.1208 & -0.0373 \end{bmatrix} \text{ and } \mathbf{T} = \begin{bmatrix} 1 & -1 \\ 3 & -2 \end{bmatrix}$$

The critical observation to be made is that $\mathbf{T}$ will typically be different depending on whether the LLL algorithm is run on $\mathbf{H}$ or $\bar{\mathbf{H}}$. As such the impact (of incorporating transmit signal scaling in the channel matrix) on the LLL algorithm must be examined.

A qualitative method of examining this impact is to examine the previously introduced orthogonal defect of reduced matrices. The simulation as described for Fig. 1 was performed on $\bar{\mathbf{H}}$ with QPSK and 64-QAM on alternate transmit antennas of a four transmit, four receive antenna system. As we can see in Fig. 3, there is a further improvement in the reduced basis orthogonality defect of scaled channel matrices.

In fact, by experimenting with varying combinations of QPSK, 16-QAM and 64-QAM on a four transmit antenna system we found that this difference was greatest when modulation formats were selected as in Fig. 3. We hypothesise that by scaling the basis vectors of the channel matrix independently, lattice reduction algorithms are better able to perform reduction, thereby reducing the mean orthogonality defect. It should be noted that it is only when basis vectors are scaled differently that a change in the orthogonality defect is observed. This is due to the fact that scaling the channel matrix by a scalar does not effect the outcome or process of lattice reduction.

5.2 Complexity Reduction

Considerable complexity reduction can be achieved in fading channels through a new technique we call Adaptive Lattice Reduction (ALR). In a slowly fading channel, the elements of $\mathbf{H}$ change slowly and are therefore correlated in time. It can be demonstrated that for these channels the transform matrix $\mathbf{T}$ is constant for several renditions of the channel. As such, a complexity reduction can be achieved by not directly recalculating the reduced basis $\mathbf{H}_{\mathrm{L}}$ every time the channel varies.

From (4) we can calculate the new reduced basis by simply multiplying a new $\mathbf{H}$ by a previously calculated $\mathbf{T}$. Even if $\mathbf{T}$ is not the optimal basis transform, the reduced basis still spans the same space as the new $\mathbf{H}$, it is simply not as orthogonal.

Furthermore, as noted in Example 1, (4) holds true after every step of the LLL algorithm. Further complexity reduction can be achieved by using a previously calculated $\mathbf{T}$ to "pre-reduce" a new $\mathbf{H}$ in order to reduce the number of steps required to compute the new reduced basis. We can simply pre-reduce a new $\mathbf{H}$ by calculating $\mathbf{H}' = \mathbf{H}\mathbf{T}^{\mathrm{A}}$, where $\mathbf{T}^{\mathrm{A}}$ is a previously calculated basis transform. The aim is that this pre-reduced basis is already closer to orthogonal and many steps of the LLL algorithm can be skipped.

To generate the new reduced basis and transform, we perform lattice reduction on the pre-reduced matrix $\mathbf{H}'$ to calculate $\mathbf{H}'_{\mathrm{L}}$. This procedure calculates a new basis transform $\mathbf{T}^{\mathrm{B}}$ such that $\mathbf{H}'_{\mathrm{L}} = (\mathbf{H}\mathbf{T}^{\mathrm{A}})\mathbf{T}^{\mathrm{B}}$. The two transforms can be combined to calculate the transform $\mathbf{T} = \mathbf{T}^{\mathrm{A}}\mathbf{T}^{\mathrm{B}}$ such that

$$\mathbf{H}'_{\mathrm{L}} = \mathbf{H}\mathbf{T} \tag{9}$$

$\mathbf{T}$ can then be used to pre-reduce the next $\mathbf{H}$. Alternatively, if the initial value $\mathbf{T}^0$ is initialised to the previous transform value $\mathbf{T}^{\mathrm{A}}$, the transform produced by the LLL algorithm will already be $\mathbf{T}$ and the explicit multiplication $\mathbf{T} = \mathbf{T}^{\mathrm{A}}\mathbf{T}^{\mathrm{B}}$ can be skipped.

Simulations have shown that progressively updating the transform matrix by using this pre-reduction technique yields a significant reduction of the number of steps needed in the LLL algorithm. We reuse the setup from Fig. 3, except this time make use of a time fading channel. We selected to base our simulations around specifications similar to that used in mobile 3GPP environments. These parameters are outlined in Table 1.

Table 1: Temporal Fading Simulation Parameters

Property	Value
Tx / Rx Antennas	4×4
Fading Type	Jakes Doppler Spectrum
Fading Method	Rice Method of Exact Doppler Spread
Carrier Frequency	2100 MHz
Sampling Frequency	1.94 MHz
Fading Period	960 received symbols successive blocks are uncorrelated.

The sampling frequency selected represents the slowest sampling frequency available in 3GPP systems. This causes the highest normalised Doppler frequency and as such can be considered a worst case.

Firstly, we varied the maximum Doppler velocity from 1km/h up to the maximum 3GPP Long Term Evolution target of 350km/h. We examined the orthogonality defect of each channel basis before reduction, after lattice reduction and after adaptive lattice reduction. As expected, the cumulative density of the orthogonality defect did not vary as the velocity was increased. Significantly, neither did that of the reduced and adaptively reduced channel basis. This confirms that the quality of basis are not based on the maximum Doppler velocity, this is somewhat intuitive as the expectation of each individual channel basis is not dependant on the time correlation introduced.

Next, in order to perform a complexity comparison, we counted the number of arithmetic operations performed by the LLL algorithm with complex additions counting as 2 and complex multiplications as 6 operations. To provide a fair comparison, we also included the cost of the pre-reduction matrix multiplication used by adaptive lattice reduction. The results proved interesting as the complexity of the adaptive scheme did not increase considerably even as the maximum Doppler velocity was increased. This is shown in Table 2 where the percentage of saved floating point operations (FLOPS) does not vary considerably, even at the high velocity of 350km/h.

Table 2: Complexity comparison between adaptive and non-adaptive lattice reduction as the maximum Doppler velocity is varied.

Velocity (km/h)	FLOPS		% saved
	LR	ALR	
10	1207	821	32.0%
60	1207	822	31.9%
120	1205	823	31.7%
350	1208	828	31.4%

We hypothesise that even though the channel does indeed vary more rapidly as the maximum Doppler velocity is increased, the rate at which $\mathbf{T}$ needs to be updated does not. This can be explained by the fact that the elements of $\mathbf{T}$ are integer-valued and as such small perturbations in $\mathbf{H}$ do not necessarily lead to changes in $\mathbf{T}$. It may therefore be acceptable in such scenarios to presume $\mathbf{T}$ static for a number of symbol periods. This therefore leads to our next simulation where we examine the effect of increasing the number of received symbols between successive channel updates.

We examined the complexity as the channel update frequency was reduced. This was performed by increasing the number of received symbols between successive channel updates, or in other words by holding the measured value of $\mathbf{H}$ static for several received symbols. This effectively increases the normalised Doppler frequency as seen by the channel reduction algorithm. This simulation was run at the maximum 3GPP target of 350km/h. As can be shown in Fig. 4, the complexity of the adaptive scheme slowly approaches that of the non-adaptive scheme. As the error rate deteriorates significantly as the channel update frequency is reduced, we can conclude that in any practical detector, adaptive lattice reduction will always offer significantly lower complexity reduction for equivalent error-rate performance.

It can be observed that when pre-reduction is used, the reduced basis and corresponding transform matrix produced is often different to that found without pre-reduction. However, the quality of the two reduced bases are on average the same. Fig. 5 shows that the cumulative density of the orthogonality defect is indistinguishable between the adaptive and unmodified reduction implementations. Therefore, it can be expected that for a given channel model and channel update frequency, adaptive lattice reduction will offer equivalent performance at lower complexity.

Finally, again as (4) holds true after every step of the LLL algorithm, the algorithm can be terminated after a pre-determined maximum number of steps. This is important as it can be used to constrain the complexity of the algorithm. This would be particularly relevant for a hardware implementation. By combining pre-reduction and early termination, the algorithm will progressively move toward the optimum reduced basis whilst capping the number of iterations performed on each rendition of $\mathbf{H}$.

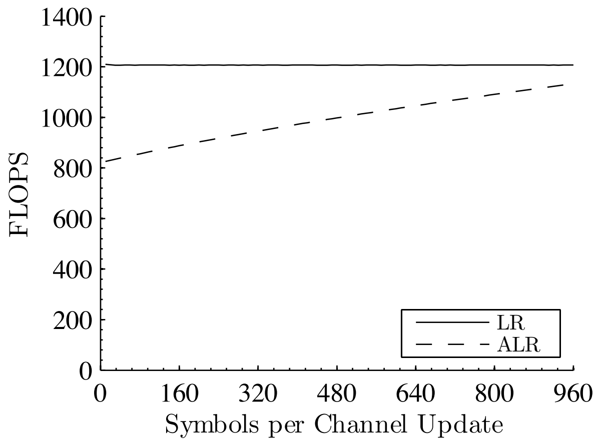

Figure 4: Complexity comparison between adaptive and non-adaptive lattice reduction as the number of symbols between channel updates is varied.

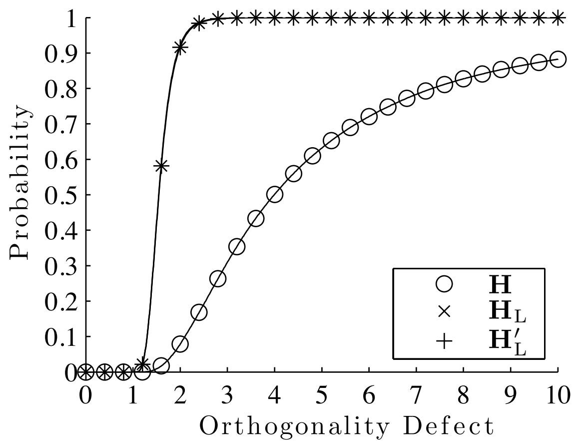

Figure 5: Cumulative density of the orthogonality defect for a correlated fading channel

6. CONCLUSION

In this paper two enhancements to LRAD have been presented which solve a critical incompatibility and considerably reduce the complexity of lattice reduction. Firstly, we have identified transmit power scaling as a potential problem for LRAD and provided a method to avoid this inherent incompatibility. While indeed a simple method to implement, we are unaware of any other work which has previously identified this inherent incompatibility and therefore believe that it is a valuable contribution for future practical implementations. Secondly, by introducing the new technique we call pre-reduction, we have shown that substantial complexity reduction can be achieved by exploiting the static nature of the LRAD transform matrix in fading channels. The newly introduced technique of pre-reduction forms the basis for our Adaptive Lattice Reduction approach. These enhancements have considerable potential for improving the performance and reducing complexity in future practical implementations of LRAD based detection schemes for MIMO communication systems.

A future study to perform a quantitative analysis of the impacts of scaling the channel on the LLL algorithm is needed. Also, it is for future study to generalise these methods to deal with the effects of MIMO precoding. Precoding also results in transmitted symbols no longer forming a subset of the integer lattice. It is intuitive that, as with symbol power scaling, any precoding step can also be modeled as a function on the channel matrix. By doing this, LRAD methods would be possible on such systems.

REFERENCES

[1] C. Windpassinger, L. Lampe, R. F. H. Fischer, and T. Hehn, “A performance study of MIMO detectors,” *IEEE Trans. Wireless Commun.*, vol. 5, no. 8, pp. 2004–2008, Aug. 2006.

[2] A. K. Lenstra, H. W. Lenstra, and L. Lovász, “Factoring polynomials with rational coefficients,” *Math. Ann.*, vol. 261, no. 4, pp. 515–534, Dec. 1982.

[3] X. Ma and W. Zhang, “Performance analysis for MIMO systems with lattice-reduction aided linear equalization,” *IEEE Trans. Commun.*, vol. 56, no. 2, pp. 309–318, Feb. 2008.

[4] P. Silvola, K. Hooli, and M. Juntti, “Suboptimal soft-output MAP detector with lattice reduction,” *IEEE Signal Process. Lett.*, vol. 13, no. 6, pp. 321–324, Jun. 2006.

[5] C. Windpassinger and R. F. H. Fischer, “Low-complexity near-maximum-likelihood detection and precoding for MIMO systems using lattice reduction,” in *Proc. IEEE Information Theory Workshop*, Paris, France, Mar. 2003, pp. 345–348.

[6] Y. H. Gan and W. H. Mow, “Complex lattice reduction algorithms for low-complexity MIMO detection,” in *Proc. IEEE GLOBECOM ’05*, St. Louis, Missouri, USA, 2005, pp. 2953–2957.

[7] H. Cohen, *A Course in Computational Algebraic Number Theory*. Berlin, Germany: Springer-Verlag, 1993.

[8] E. Agrell, T. Eriksson, A. Vardy, and K. Zeger, “Closest point search in lattices,” *IEEE Trans. Inf. Theory*, vol. 48, no. 8, pp. 2953–2957, Aug. 2002.

[9] C. Windpassinger, “Detection and precoding for multiple input multiple output channels,” Ph.D. dissertation, Universität Erlangen-Nürnberg, Germany, 2004.

[10] W. H. Mow, “Universal lattice decoding: principle and recent advances,” *Wirel. Commun. Mob. Comput.*, vol. 3, no. 5, pp. 553–569, Aug. 2003.